



Active and passive earth pressure coefficients by a kinematical approach

A.-H. Soubra and B. Macuh

A simple method is proposed for calculating the active and passive earth pressure coefficients in the general case of an inclined wall and a sloping backfill. The approach used is based on rotational log-spiral failure mechanisms in the framework of the upper-bound theorem of limit analysis. It is shown that the energy balance equation of a rotational log-spiral mechanism is equivalent to the moment equilibrium equation about the centre of the log-spiral. Numerical optimisation of the active and passive earth pressure coefficients is performed automatically by a spreadsheet optimisation tool. The implementation of the proposed method is illustrated using an example. The predictions by the present method are compared with those given by other authors.

NOTATION

c	cohesion
dl	elementary length along the slip surface BC
\dot{D}	rate of energy dissipation
f_1, f_2, \dots, f_8	intermediate non-dimensional functions
K_γ, K_q, K_c	earth pressure coefficients due to soil weight, vertical surcharge loading and cohesion
$K_{a\gamma}, K_{aq}, K_{ac}$	active earth pressure coefficients
$K_{p\gamma}, K_{pq}, K_{pc}$	passive earth pressure coefficients
K_{aq0}, K_{pq0}	active and passive earth pressure coefficients due to a surcharge loading normal to the ground surface
l/r_0 and L/r_0	intermediate non-dimensional functions
l	wall length
L	length of AB
P_a, P_p	active and passive forces respectively
P_{ad}	adhesive force
q	vertical surcharge loading
q_0	surcharge loading normal to the ground surface
r_0, r_1	initial and final radius of the log-spiral slip surface
V	velocity at the velocity discontinuity
W	weight of the soil mass ABC
\dot{W}	rate of work of an external force
α	inclination of the Rankine earth pressure
β	slope of the backfill
γ	unit weight of the soil

δ	friction angle at the soil–structure interface
θ_0, θ_1	angles defining the log-spiral slip surface
λ	angle between the soil–wall interface and the vertical direction
ξ	inclination of the Rankine slip surface with the horizontal direction
σ	normal stress acting on the slip surface
τ	tangential stress acting on the slip surface
ϕ	angle of internal friction of the soil
Ω	angular velocity of failure mechanism

1. INTRODUCTION

The problem of active and passive earth pressures acting against rigid retaining structures has been extensively studied in the literature since Coulomb.¹ Most of the existing methods are based on either the limit equilibrium method, the slip line method or the limit analysis method.

Recently, a variational analysis has been applied to the passive earth pressure problem by Soubra *et al.*² Their approach is based on a limit equilibrium method, and the solution provides a log-spiral failure surface. For their failure wedge, the moment equilibrium equation can be used for the calculation of the passive earth pressures without specifying the normal stress distribution along the log-spiral slip surface. It should be emphasised that their method, employed in this paper, can be categorised also as an upper-bound in the framework of limit analysis where a rotational rigid body movement is considered. This variational limit equilibrium method may be easily extended to the active earth pressure problem, and the same conclusions remain valid in this case:

- A log-spiral failure surface may be obtained from a variational maximisation procedure.
- The moment equilibrium equation, which is equivalent to the energy balance equation in the framework of the upper-bound method of limit analysis, may be used for computation of the active earth pressures.

The aim of this paper is to show that the upper-bound method in limit analysis for a rotational log-spiral failure mechanism gives rapid and good predictions for both active and passive earth pressures. It is also demonstrated that the present method can be easily implemented on a PC by defining spreadsheet

functions and by using a powerful spreadsheet optimisation tool. The analysis is made in the general case of an inclined wall and a sloping backfill, and considers a frictional and cohesive (c, ϕ) soil. A uniform surcharge is assumed to act on the ground surface. Active and passive earth pressure coefficients due to soil weight, cohesion and surcharge loading are presented for various governing parameters and compared with those given by other authors.

2. FAILURE MECHANISMS AND GOVERNING EQUATIONS

The variational analysis details and the equivalence between the variational limit equilibrium method and the upper-bound method in limit analysis for a rotational log-spiral failure mechanism are given elsewhere.² However, for clarity, only the upper-bound technique (that is, the kinematical approach) of limit analysis is briefly described here.

Two rotational log-spiral failure mechanisms are considered in the present analysis, one for the active state M1 (Fig. 1(a)) and the other for the passive state M2 (Fig. 1(b)). For both M1 and M2 mechanisms, the region ABC rotates as a rigid body about the as yet undefined centre of rotation O relative to the material below the logarithmic failure surface BC. Thus the

surface BC is a surface of velocity discontinuity. These failure mechanisms can be specified completely by two variables θ_0 and θ_1 . It should be emphasised that the earth pressure coefficient due to soil weight, K_γ , is calculated with the assumption of a cohesionless soil with no surcharge loading. The computation of the coefficients K_q and K_c due to surcharge loading and cohesion is based on the assumption of a weightless soil with $c = 0$ for K_q and $q = 0$ for K_c . The formulation for the coefficients of earth pressure due to soil weight, surcharge and cohesion follows.

2.1. Rate of work of external forces

As shown in Fig. 1, the external forces acting on the soil mass in motion consist of the self-weight of the soil, W , the active or passive earth force (P_a or P_p), the adhesive force, $P_{ad}(= cl \tan \delta / \tan \phi)$, and the surcharge, qL , acting on the ground surface. The rate of work for the different external forces can be calculated as follows.

2.1.1. Rate of work of the soil weight. A direct integration of the rate of work of the soil weight in the region ABC is very complicated. An easier alternative is first to find the rate of work \dot{W}_{OBC} , \dot{W}_{OAB} and \dot{W}_{OAC} due to soil weight in the regions OBC, OAB and OAC respectively. The rate of work for the

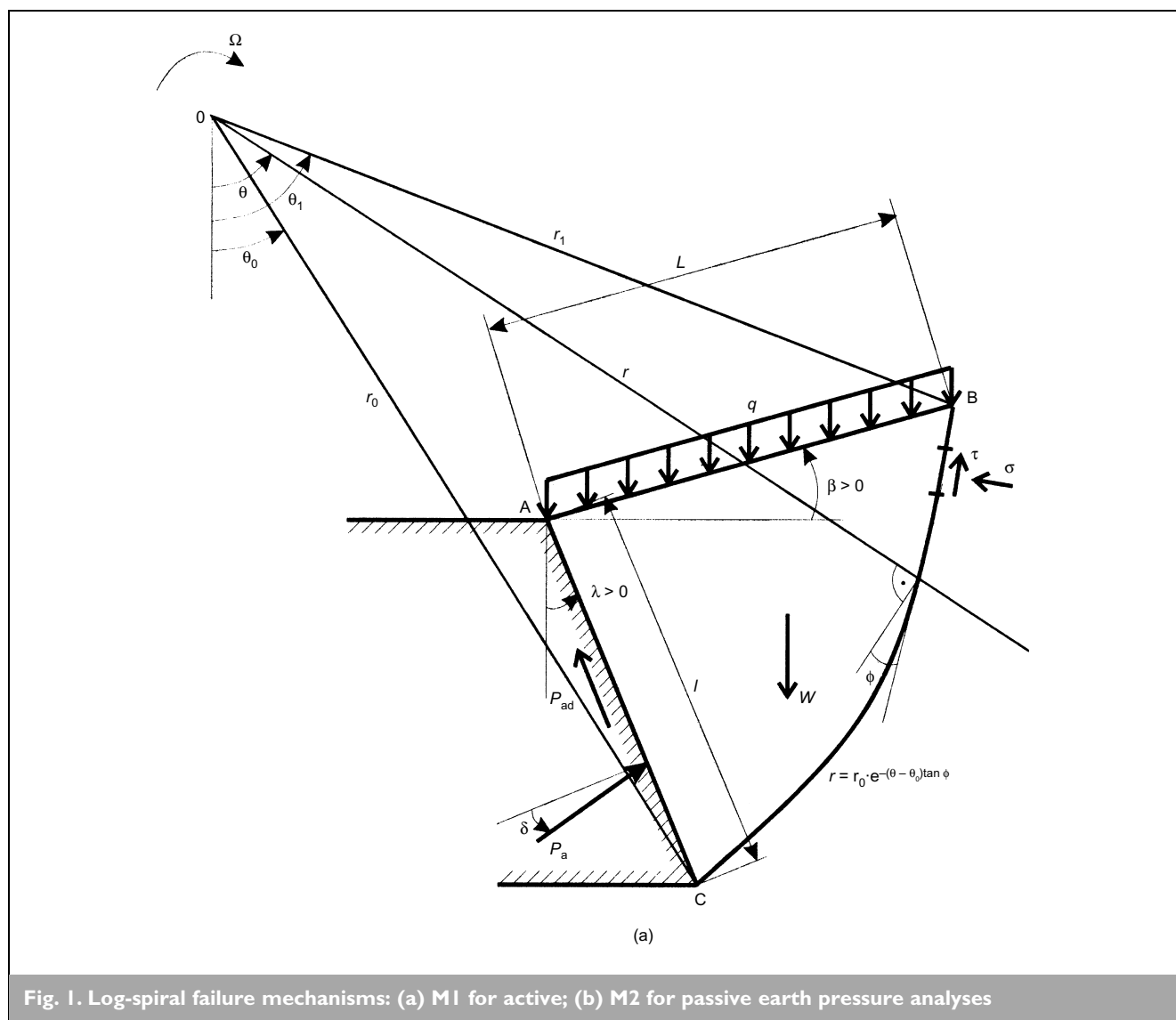


Fig. 1. Log-spiral failure mechanisms: (a) M1 for active; (b) M2 for passive earth pressure analyses

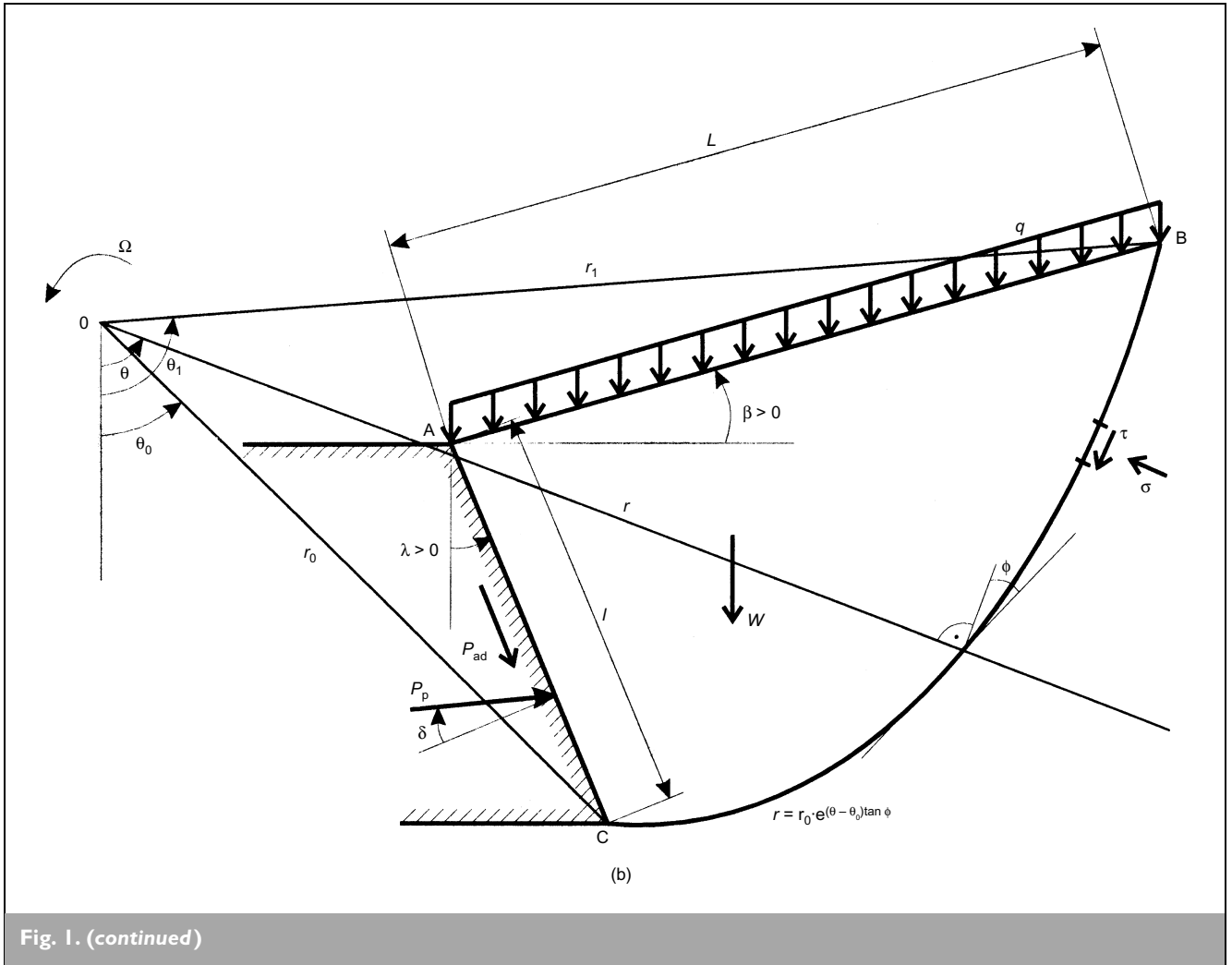


Fig. 1. (continued)

region ABC is then found by simple algebraic summation, $\dot{W}_{OBC} - \dot{W}_{OAB} - \dot{W}_{OAC}$. The steps of computation of the rate of work due to self-weight of the soil are essentially the same as those of an inclined slope considered by Chen.³ It is found that the rate of work due to the soil weight in the region ABC is

1	$\dot{W}_{\text{soil}} = \gamma r_0^3 \Omega (f_1 - f_2 - f_3)$
---	---

where f_1 , f_2 and f_3 are non-dimensional functions, which are given in Appendix 1.

2.1.2. Rate of work of the active or passive force and the adhesive force. The rate of work of the active or passive force (P_a or P_p) and the adhesive force, P_{ad} , can be expressed as follows:

2	$\dot{W}_{(P_a \text{ or } P_p), P_{ad}} = P_{a,p} r_0 \Omega f_4 + c r_0^2 \Omega f_5$
---	---

where f_4 and f_5 are non-dimensional functions, which are given in Appendix 1. It should be mentioned that the active or passive force is assumed to act at the lower third of the wall length for the calculation of the coefficients K_{ay} and K_{py} . However, the computation of K_{ac} , K_{pc} , K_{aq} and K_{pq} is based on the assumption that the point of application of the active or passive force is applied at the middle of the wall length. These

hypotheses are in conformity with the classical earth pressure distributions, and allow direct comparison with existing solutions.

2.1.3. Rate of work of the surcharge loading. The rate of work of the surcharge loading q can be expressed as follows:

3	$\dot{W}_q = q r_0^2 \Omega f_6$
---	----------------------------------

where f_6 is a non-dimensional function, which is given in Appendix 1.

The total rate of work of the external forces is the summation of these three contributions—that is, equations (1), (2) and (3):

4	$\sum [\dot{W}]_{\text{ext}} = \dot{W}_{\text{soil}} + \dot{W}_{(P_a \text{ or } P_p), P_{ad}} + \dot{W}_q$
---	---

2.2. Rate of energy dissipation

Since no general plastic deformation of the soil is permitted to occur, the energy is dissipated solely at the velocity discontinuity surface BC between the material at rest and the material in motion. The rate of energy dissipation per unit area of a velocity discontinuity can be expressed as³

5

$$\dot{D} = cV \cos \phi$$

where V is the velocity that makes an angle ϕ with the velocity discontinuity. The total rate of energy dissipation along BC can be expressed as follows:

6

$$\dot{D}_{BC} = cr_0^2 \Omega f_7$$

where f_7 is a non-dimensional function, which is given in Appendix 1.

2.3. Energy balance equation

By equating the total rate of work of external forces (equation (4)) to the total rate of energy dissipation (equation (6)), we have

7

$$\gamma r_0^3 (f_1 - f_2 - f_3) + P_{a,p} r_0 f_4 + cr_0^2 f_5 + qr_0^2 f_6 = cr_0^2 f_7$$

The energy balance equation of the rotational log-spiral mechanism (i.e. equation (7)) is identical to the moment equilibrium equation about the centre of the log-spiral. It should be emphasised that the log-spiral function has a particular property, that the resultant of the forces ($\sigma \cdot dl$) and ($\tan \phi \cdot \sigma \cdot dl$) passes through the pole of the spiral. Hence the moment equilibrium equation of the soil mass in motion about the centre of the log-spiral is independent of the normal stress distribution along the slip surface. Based on equation (7), the active and passive forces can be expressed respectively as follows:

8

$$P_a = K_{ay} \frac{\gamma l^2}{2} + K_{aq} ql - K_{ac} cl$$

9

$$P_p = K_{py} \frac{\gamma l^2}{2} + K_{pq} ql + K_{pc} cl$$

where K_{ay} , K_{py} , K_{aq} , K_{pq} , K_{ac} and K_{pc} are the earth pressure coefficients. The coefficients K_γ , K_q and K_c represent respectively the effect of soil weight, vertical surcharge loading and cohesion, and the subscripts a and p represent the active and passive cases respectively. These coefficients are given as follows, using the lower sign for the passive case:

10

$$-K_{ay} = K_{py} = \frac{2}{\left(\frac{l}{r_0}\right)^2} \cdot \frac{(f_1 - f_2 - f_3)}{f_4}$$

11

$$-K_{aq} = K_{pq} = \frac{1}{r_0} \cdot \frac{f_6}{f_4}$$

12

$$K_{ac,pc} = \mu \frac{1}{r_0} \frac{f_7 - f_5}{f_4}$$

For a surcharge loading q_0 normal to the ground surface, the active and passive earth pressure coefficients, K_{aq0} and K_{pq0} , are given as follows:

13

$$K_{aq0,pq0} = \pm \frac{1}{r_0} \cdot \frac{f_8}{f_4}$$

where f_8 is a non-dimensional function, which is given in Appendix 1.

3. NUMERICAL RESULTS

The most critical earth pressure coefficients can be obtained by numerical maximisation of the coefficients K_{ay} , K_{aq} and K_{aq0} and minimisation of the coefficients K_{ac} , K_{py} , K_{pq} , K_{pq0} and K_{pc} . These optimisations are made with regard to the parameters θ_0 and θ_1 . The procedure can be performed using the optimisation tool available in most spreadsheet software packages. In this paper the Solver optimisation tool of Microsoft Excel has been used. Two computer programs have been developed using Visual Basic for Applications (VBA) to define the active and passive earth pressure coefficients as functions of the two angular parameters θ_0 and θ_1 defined in Fig. 1.

In the following sections, the passive and active earth pressure coefficients obtained from the present analysis are presented and compared with those given by other authors. Then a demonstration of the implementation of earth pressure coefficients as user-defined functions in Microsoft Excel Visual Basic is presented. An illustrative example shows the easy use of spreadsheets in optimisation problems. The paper ends with the presentation of two design tables giving some values of the active and passive earth pressure coefficients for practical use in geotechnical engineering.

3.1. Passive earth pressure coefficients

There are a great many solutions for the passive earth pressure problem in the literature based on

- the limit equilibrium method⁴⁻¹⁵
- the slip line method¹⁶⁻²⁰
- limit analysis theory.^{2, 21-28}

The tendency today in practice is to use the values given by Kérisel and Absi.²⁹

3.1.1. Comparison with Rankine solution. For the general case of an inclined wall and a sloping backfill ($\lambda/\phi \neq 0$, $\beta/\phi \neq 0$), the Rankine passive earth pressure is inclined at an angle α with the normal to the wall irrespective of the angle of friction at the soil-wall interface,³⁰ where

14

$$\tan \alpha = \frac{\sin(\omega_\beta + \beta - 2\lambda)\sin \phi}{1 + \sin \phi \cos(\omega_\beta + \beta - 2\lambda)}$$

and

$$15 \quad \sin \omega_\beta = \frac{\sin \beta}{\sin \phi}$$

The inclination of the slip surface with the horizontal direction is given as follows:

$$16 \quad \xi = \frac{\omega_\beta + \beta}{2} + \frac{\pi}{4} - \frac{\phi}{2}$$

and the coefficient K_{py} is given by

$$17 \quad K_{py} = \frac{\cos(\lambda - \beta) \sin \omega_\beta}{\cos \alpha \sin(\omega_\beta - \beta)} [1 + \sin \phi \cos(\omega_\beta + \beta - 2\lambda)]$$

In order to validate the results of the present analysis, one considers a soil-wall friction angle δ equal to the α value given by equation (14). The numerical solutions obtained by the computer program have shown that, in these cases, the present results are similar to the exact solutions given by Rankine (that is, equations (16) and (17)); the log-spiral slip surface degenerates to a planar surface with radii approaching infinity.

It should be emphasised that the results obtained from the computer program indicate that the coefficient K_{pc} is related to the coefficient K_{pq0} by the following relationship (cf. Caquot's theorem of corresponding states³¹):

$$18 \quad K_{pc} = \frac{K_{pq0} - \frac{1}{\cos \delta}}{\tan \phi}$$

Also, it should be mentioned that the critical angular parameters θ_0 and θ_1 obtained from the minimisation of both K_{pq0} and K_{pc} give exactly the same critical geometry.

3.1.2. Comparison with Kérisel and Absi. Figures 2 and 3 show the comparison of the present solutions of K_{py} and K_{pq} with those of Kérisel and Absi²⁹ for the case of a vertical wall and an inclined backfill, and for the case of an inclined wall and a horizontal backfill respectively, when $\phi = 40^\circ$.

For the K_{py} coefficient, the present results are greater than those of Kérisel and Absi. However, the maximum difference does not exceed 13%. For the K_{pq} coefficient, the present solutions continue to be greater than those of Kérisel and Absi; a maximum difference of 22% is obtained for the extreme case when $\phi = 40^\circ$, $\delta/\phi = 1$, $\beta/\phi = 0$ and $\lambda = -30^\circ$.

To conclude, the present solutions of K_{py} and K_{pq} are greater than the ones given by Kérisel and Absi. However, for practical configurations ($\phi \leq 40^\circ$, $1/3 \leq \delta/\phi \leq 2/3$, $\beta/\phi \leq 1/3$ and $\lambda = 0^\circ$), the maximum difference does not exceed 5% for K_{py} and 7% for K_{pq} .

3.1.3. Comparison with the existing upper-bound solutions. Rigorous upper-bound solutions of the passive earth

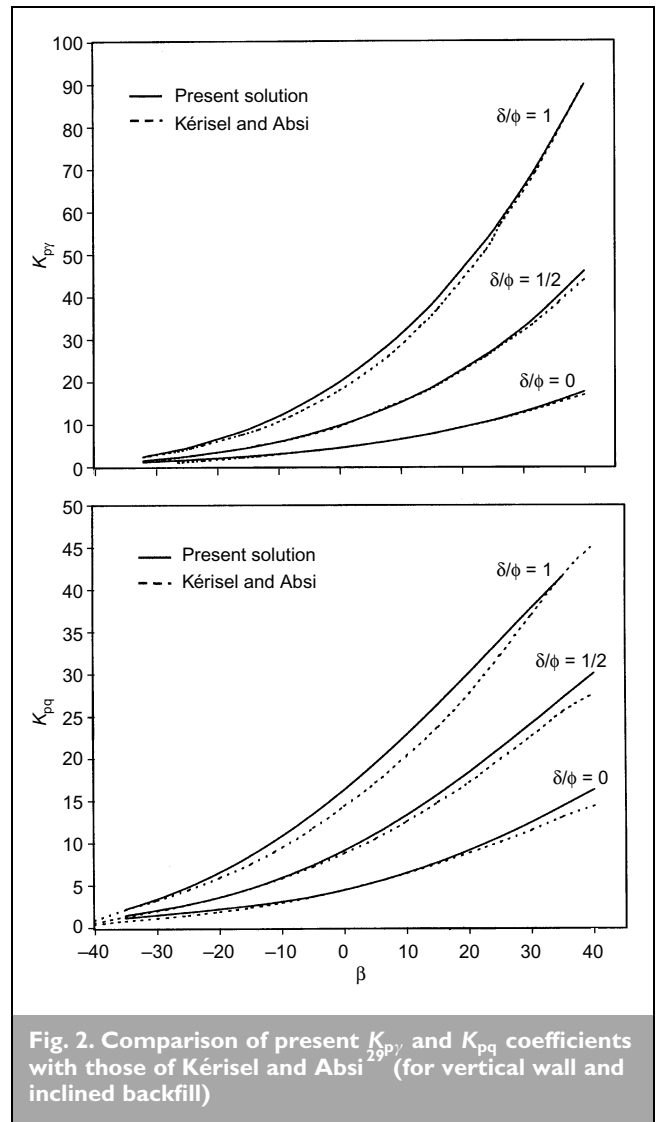


Fig. 2. Comparison of present K_{py} and K_{pq} coefficients with those of Kérisel and Absi²⁹ (for vertical wall and inclined backfill)

pressure problem are proposed in the literature by Chen and Rosenfarb²³ and Soubra.²⁷ Chen and Rosenfarb considered six translational failure mechanisms and showed that the log-sandwich mechanism gives the least (that is, the best) upper-bound solutions. Recently, Soubra²⁷ considered a translational multiblock failure mechanism and improved significantly the existing upper-bound solutions given by the log-sandwich mechanism for the K_{py} coefficient, since he obtained smaller upper bounds. The improvement (that is, the reduction relative to Chen and Rosenfarb's upper-bound solution) attains 21% when $\phi = 45^\circ$, $\delta/\phi = 1$, $\beta/\phi = 1$ and $\lambda = -15^\circ$.

The results of K_{py} and K_{pq} given by the present rotational failure mechanism and those given by Soubra²⁷ using a translational failure mechanism are presented in Fig. 4 for the general case of an inclined wall and a sloping backfill when $\phi = 45^\circ$ and $\delta/\phi = 1$.

For the K_{py} coefficient, the present upper-bound solutions are smaller (that is, better) than those of Soubra.²⁷ The improvement (that is, the reduction relative to Soubra's upper-bound solution) is 27% when $\phi = 45^\circ$, $\delta/\phi = 1$, $\beta/\phi = 1$ and $\lambda = -15^\circ$. For the K_{pq} coefficient, it should be mentioned that the values obtained by Soubra²⁷ are identical to those given by Kérisel and Absi²⁹ and correspond to the exact solutions for a

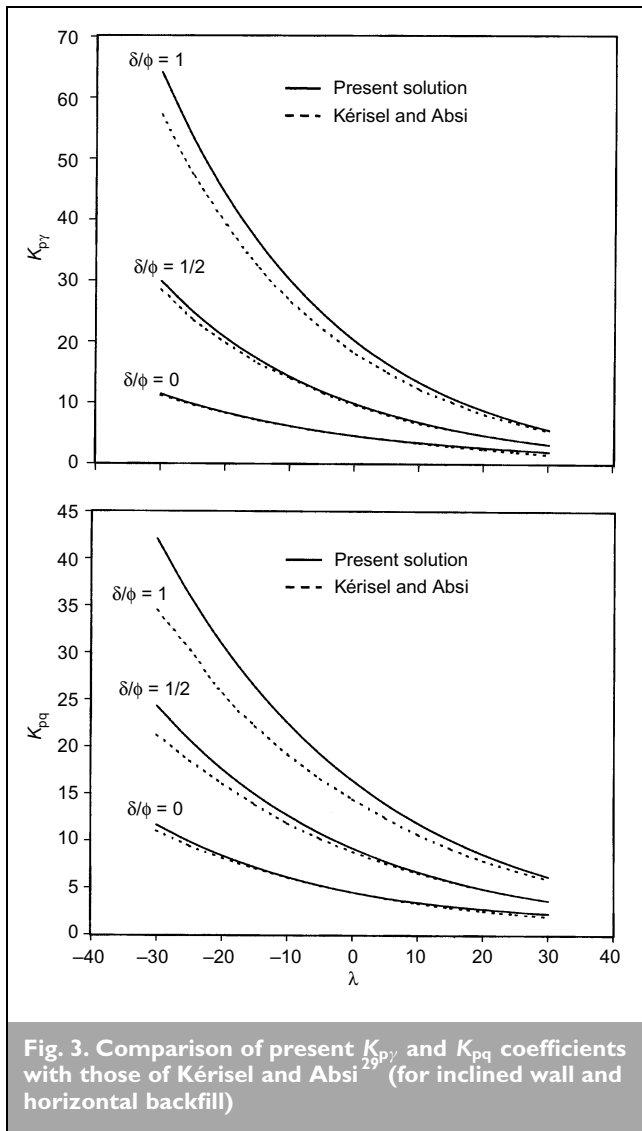


Fig. 3. Comparison of present K_{py} and K_{pq} coefficients with those of Kérisel and Absi²⁹ (for inclined wall and horizontal backfill)

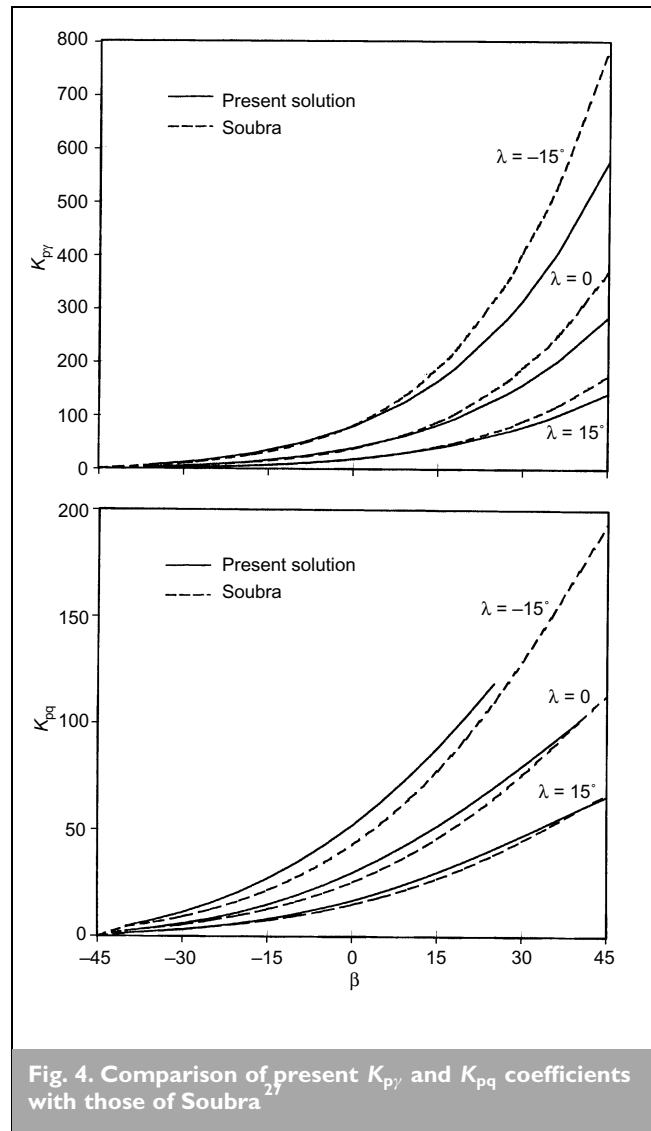


Fig. 4. Comparison of present K_{py} and K_{pq} coefficients with those of Soubra²⁷

weightless soil. The present upper-bound solutions of the K_{pq} coefficient are greater than those of Soubra²⁷ and thus overestimate the exact solutions. However, for practical configurations ($\phi \leq 40^\circ$, $1/3 \leq \delta/\phi \leq 2/3$, $\beta/\phi \leq 1/3$ and $\lambda = 0^\circ$) the maximum difference does not exceed 7.5%.

3.2. Active earth pressure coefficients

As in the case of passive earth pressures, the numerical solutions obtained by the computer program have shown that the present model gives the exact solutions proposed by Rankine (when they exist). In these cases, the log-spiral slip surface degenerates to a planar surface with radii approaching infinity. Also, it should be mentioned that the following relationship between K_{ac} and K_{aq0} is valid in the present analysis:

$$K_{ac} = \frac{1}{\cos \delta} - K_{aq0} \tan \phi$$

and that the calculation of K_{aq0} and K_{ac} gives exactly the same critical geometry.

3.2.1. Comparison with Kérisel and Absi. Figures 5 and 6 show the comparison of the present solutions of K_{ay} and K_{aq}

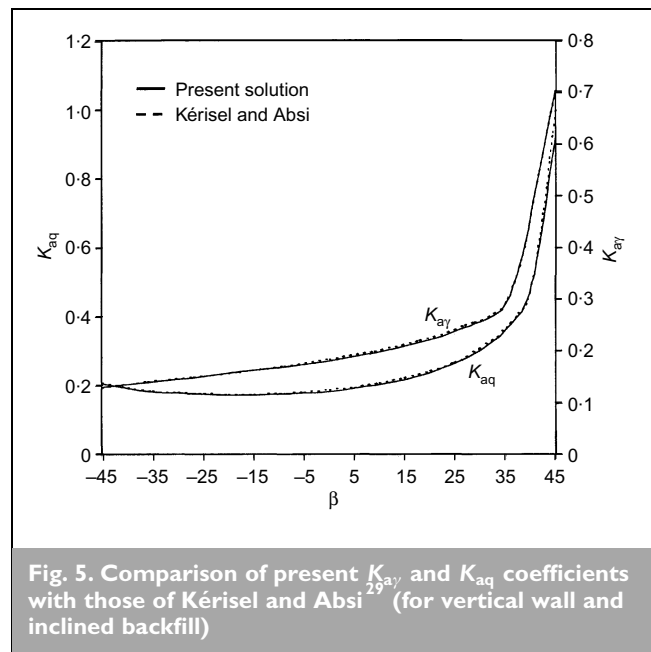


Fig. 5. Comparison of present K_{ay} and K_{aq} coefficients with those of Kérisel and Absi²⁹ (for vertical wall and inclined backfill)

with those of Kérisel and Absi²⁹ in the case of a vertical wall and an inclined backfill, and in the case of an inclined wall and a horizontal backfill respectively, when $\phi = 45^\circ$ and $\delta/\phi = 1$.

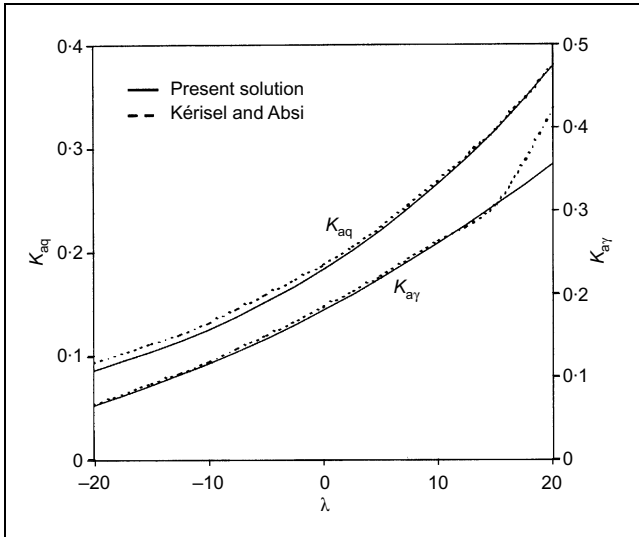


Fig. 6. Comparison of present K_{ay} and K_{aq} coefficients with those of Kérisel and Absi²⁹ (for inclined wall and horizontal backfill)

The present results are smaller than those of Kérisel and Absi. For the K_{ay} coefficient, the maximum difference does not exceed 3% when $\lambda \leq 15^\circ$; however, for $\lambda = 20^\circ$ a significant difference is observed. After careful examination of the values proposed by Kérisel and Absi for similar configurations (see for instance their values for $\delta/\phi = 0.66$ or 0), it seems that their K_{ay} value for $\phi = 45^\circ$, $\delta/\phi = 1$, $\beta = 0^\circ$ and $\lambda = 20^\circ$ is not correct. For the K_{aq} coefficient the underestimation does not exceed 8%.

The preceding comparisons allow one to conclude that, for practical configurations ($\phi \leq 40^\circ$, $\delta/\phi \leq 1$, $\beta/\phi \geq -1/3$ and $\lambda = 0^\circ$), there is good agreement with the currently used results of Kérisel and Absi for both K_{ay} and K_{aq} . The maximum difference does not exceed 3%.

4. IMPLEMENTATION OF USER-DEFINED FUNCTIONS IN VISUAL BASIC FOR APPLICATIONS, AND THE USE OF SOLVER

To implement the functions defining the passive earth pressure coefficients and to run the Solver optimisation tool of Microsoft Excel, one has to follow the following steps (for the active case, see the appropriate equations given in Appendix 1):

- (a) Create the user-defined functions shown in Appendix 2. This is done in Microsoft Excel 97 by first clicking Tools/Macro/Visual Basic Editor and then clicking Insert/

Module and, in the module sheet, typing 'Option explicit ...', etc. The functions are simple and self-explanatory.

- (b) As shown in Fig. 7, cells C5, C6, C7 and C8 are input data that define the mechanical and geometrical parameters ϕ , δ , λ and β . Cells C12 and C13 contain values of angular parameters of the log-spiral slip surface θ_0 and θ_1 . Finally, cell C19 contains the formula to compute the passive earth pressure coefficient K_{py} . Arbitrary values were initially entered in cells C12 and C13 for θ_0 and θ_1 , say 0.5 for θ_0 and 1.5 for θ_1 .
- (c) Invoke the Solver tool by clicking Tools/Solver. Fig. 8 shows the Solver dialog box. To calculate the K_{py} coefficient, set the C19 cell 'equal to' minimum, 'by changing' cells C12 and C13, namely θ_0 and θ_1 , 'subject to' the constraints that C13 \geq C12 + 0.0001 ($\theta_1 > \theta_0$), C12 \leq 3.14 ($\theta_0 \leq \pi$), C13 \leq 3.14 ($\theta_1 \leq \pi$), C13 \geq 0 ($\theta_1 \geq 0$) and C19 \geq 0 ($K_{py} \geq 0$).

If Solver reports a converged solution, one should accept the solution and re-invoke Solver, until it reports it has 'found a solution'. It should be mentioned that the initial values of θ_0 and θ_1 may influence the ability of the Solver to find a solution. This need for judicious choice of starting values of θ_0 and θ_1 is not a major inconvenience because different starting values can be tried with ease using the proposed spreadsheet approach. The appealing feature of the spreadsheet approach is that once the spreadsheet is set up as shown in Fig. 7, running other problems with different geometry and soil properties merely requires changing the input data (that is, ϕ , δ , β and λ).

4.1. Illustrative example

Consider the following characteristics: $\phi = 40^\circ$, $\delta/\phi = 2/3$, $\beta/\phi = 0$ and $\lambda = 0^\circ$. Initial values of θ_0 and θ_1 are arbitrarily chosen, say 0.5 for θ_0 and 1.5 for θ_1 . Fig. 7 shows the critical coefficient $K_{py} = 12.59$ and the corresponding critical slip surface.

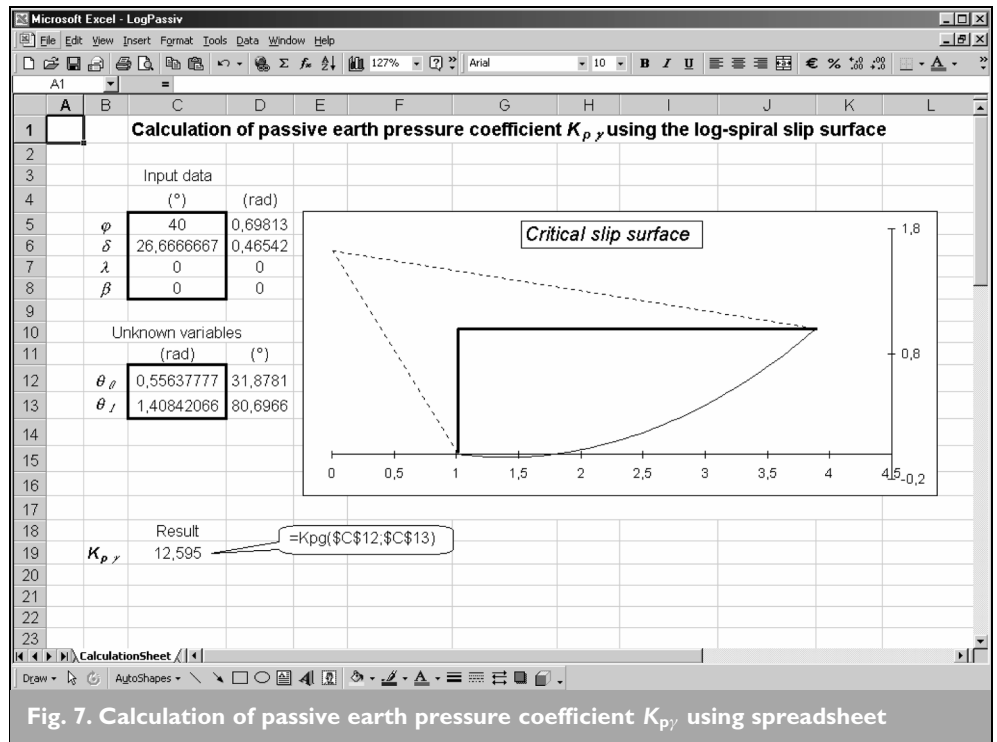


Fig. 7. Calculation of passive earth pressure coefficient K_{py} using spreadsheet

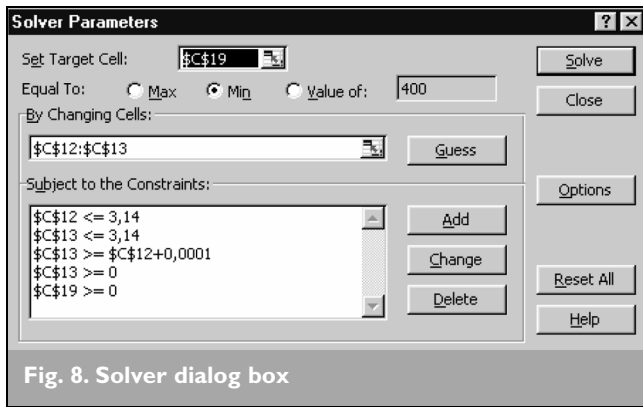


Fig. 8. Solver dialog box

5. DESIGN TABLES

Tables 1 and 2 present the coefficients K_{py} , K_{pq} , K_{pc} , K_{ay} , K_{aq} and K_{ac} obtained from the computer programs for practical use in geotechnical engineering. These values are given for ϕ ranging from 20° to 40° , for five values of δ/ϕ , for $\lambda = 0^\circ$ and for four values of β/ϕ . For practical configurations, the passive (or active) earth pressure coefficients are given for negative (or positive) β values.

6. CONCLUSIONS

A simple method using spreadsheet software has been proposed for computing the active and passive earth pressure coefficients. The method is based on the upper-bound theorem of limit analysis. The failure mechanism is of the rotational type. It is bounded by a log-spiral slip surface. The energy balance equation is shown to be equivalent to the moment equilibrium equation about the centre of the log-spiral. The present approach gives rigorous solutions for the active and passive earth pressures in the framework of the kinematical approach of limit analysis.

Numerical optimisation is performed automatically by a spreadsheet optimisation tool. The implementation of the proposed method has been illustrated using an example. Once the spreadsheet has been set up, the same template can be used for analysing other problems merely by changing the input data. The advantage of this method is its simplicity in use.

Comparison with the currently used solutions of Kérisel and Absi²⁹ leads to the following conclusions:

- For the passive case, the present solutions of K_{py} and K_{pq} are greater than those given by Kérisel and Absi.²⁹ However, for practical configurations ($\phi \leq 40^\circ$, $1/3 \leq \delta/\phi \leq 2/3$, $\beta/\phi \leq 1/3$ and $\lambda = 0^\circ$), the maximum difference does not exceed 5% for K_{py} and 7% for K_{pq} .
- For the active case, the present solutions of K_{ay} and K_{aq} allow one to conclude that for practical configurations ($\phi \leq 40^\circ$, $\delta/\phi \leq 1$, $\beta/\phi \geq -1/3$ and $\lambda = 0^\circ$), there is good agreement with the currently used results of Kérisel and Absi. The maximum difference does not exceed 3%.

On the other hand, the present analysis improves the best upper-bound solutions given in the literature by Soubra²⁷ for the K_{py} coefficient. The improvement (that is, the reduction relative to Soubra's upper-bound solution) is 27% when $\phi = 45^\circ$, $\delta/\phi = 1$, $\beta/\phi = 1$ and $\lambda = -15^\circ$. For the K_{pq}

coefficient, the present analysis overestimates the upper-bound solutions given by Soubra. However, for practical configurations ($\phi \leq 40^\circ$, $1/3 \leq \delta/\phi \leq 2/3$, $\beta/\phi \leq 1/3$ and $\lambda = 0^\circ$) the maximum difference does not exceed 7.5%.

Numerical results of the active and passive earth pressure coefficients are given in a tabular form for practical use. The proposed method, being simple and rigorous, may be an attractive alternative to other existing solutions, and can be easily extended to other stability problems in geotechnical engineering.

APPENDIX I

The non-dimensional functions f_1, f_2, \dots, f_8 are given as follows, using the lower sign for the passive case:

20

$$f_1 = \pm \frac{\mu e^{\mu 3(\theta_1 - \theta_0) \tan \phi} (3 \tan \phi \cdot \sin \theta_1 \pm \cos \theta_1)}{\pm 3 \tan \phi \cdot \sin \theta_0 + \cos \theta_0} \frac{1}{3(9 \tan^2 \phi + 1)}$$

21

$$f_2 = \pm \frac{1}{6} \frac{L}{r_0} \left(2 \sin \theta_0 - 2 \frac{l}{r_0} \sin \lambda + \frac{L}{r_0} \cos \beta \right) \cdot \cos(\theta_1 - \beta) \cdot e^{\mp(\theta_1 - \theta_0) \tan \phi}$$

22

$$f_3 = \pm \frac{1}{6} \frac{l}{r_0} \sin(\theta_0 - \lambda) \cdot \left(2 \sin \theta_0 - \frac{l}{r_0} \sin \lambda \right)$$

23

$$f_4 = \begin{cases} \cos(\delta \pm \lambda) \left(\cos \theta_0 - \frac{1}{3} \frac{l}{r_0} \cos \lambda \right) \\ \pm \sin(\delta \pm \lambda) \left(\sin \theta_0 - \frac{1}{3} \frac{l}{r_0} \sin \lambda \right) \\ \text{for } K_\lambda \\ \cos(\delta \pm \lambda) \left(\cos \theta_0 - \frac{1}{2} \frac{l}{r_0} \cos \lambda \right) \\ \pm \sin(\delta \pm \lambda) \left(\sin \theta_0 - \frac{1}{2} \frac{l}{r_0} \sin \lambda \right) \\ \text{for } K_q, K_{q0} \text{ and } K_c \end{cases}$$

24

$$f_5 = \frac{l \tan \delta}{r_0 \tan \phi} \cdot \sin(\lambda - \theta_0)$$

25

$$f_6 = \mp \frac{L}{r_0} \left(-\sin \theta_0 + \frac{l}{r_0} \sin \lambda - \frac{1}{2} \frac{L}{r_0} \cos \beta \right)$$

26

$$f_7 = \mp \frac{1}{2 \tan \phi} (e^{\mp 2(\theta_1 - \theta_0) \tan \phi} - 1)$$

ϕ	$K_{p\gamma}$					K_{pq}					K_{pc}					
	β/ϕ	0	1/3	δ/ϕ 1/2	2/3	1	0	1/3	δ/ϕ 1/2	2/3	1	0	1/3	δ/ϕ 1/2	2/3	1
20	0	2.04	2.39	2.57	2.75	3.13	2.04	2.38	2.54	2.70	3.00	2.86	3.76	4.18	4.59	5.31
	-1/3	1.71	1.94	2.07	2.21	2.49	1.72	1.96	2.09	2.21	2.46	2.43	3.21	3.59	3.94	4.57
	-1/2	1.55	1.73	1.83	1.94	2.16	1.58	1.75	1.85	1.96	2.18	2.24	2.96	3.31	3.64	4.23
	-2/3	1.39	1.51	1.58	1.66	1.83	1.43	1.55	1.62	1.70	1.87	2.07	2.72	3.05	3.36	3.91
25	0	2.46	3.07	3.41	3.76	4.54	2.46	3.04	3.34	3.65	4.24	3.14	4.36	4.98	5.58	6.74
	-1/3	1.94	2.32	2.54	2.77	3.30	1.96	2.34	2.56	2.79	3.26	2.51	3.50	4.02	4.52	5.47
	-1/2	1.71	1.97	2.13	2.31	2.72	1.75	2.02	2.18	2.37	2.75	2.26	3.13	3.59	4.05	4.91
	-2/3	1.47	1.65	1.75	1.88	2.17	1.54	1.72	1.83	1.96	2.26	2.03	2.78	3.20	3.62	4.39
30	0	3.00	4.03	4.65	5.34	6.93	3.00	3.98	4.53	5.10	6.28	3.46	5.14	6.05	6.99	8.88
	-1/3	2.20	2.77	3.14	3.56	4.54	2.24	2.82	3.18	3.57	4.44	2.59	3.84	4.54	5.26	6.71
	-1/2	1.87	2.25	2.50	2.80	3.52	1.93	2.33	2.59	2.89	3.58	2.26	3.29	3.91	4.54	5.80
	-2/3	1.55	1.79	1.94	2.13	2.62	1.65	1.90	2.07	2.27	2.76	1.97	2.83	3.35	3.89	4.99
35	0	3.69	5.44	6.59	7.95	11.30	3.69	5.35	6.34	7.42	9.82	3.84	6.18	7.55	9.05	12.28
	-1/3	2.50	3.35	3.95	4.67	6.53	2.55	3.43	4.02	4.70	6.31	2.66	4.21	5.18	6.23	8.50
	-1/2	2.03	2.57	2.96	3.44	4.70	2.13	2.70	3.10	3.59	4.79	2.23	3.46	4.26	5.13	7.02
	-2/3	1.62	1.93	2.15	2.43	3.22	1.76	2.10	2.34	2.65	3.47	1.89	2.85	3.48	4.20	5.75
40	0	4.60	7.62	9.81	12.60	20.01	4.60	7.42	9.27	11.40	16.43	4.29	7.62	9.77	12.26	18.02
	-1/3	2.83	4.10	5.09	6.35	9.93	2.91	4.22	5.20	6.39	9.42	2.70	4.66	6.00	7.56	11.21
	-1/2	2.20	2.95	3.53	4.30	6.55	2.34	3.14	3.75	4.55	6.69	2.19	3.62	4.66	5.88	8.75
	-2/3	1.67	2.08	2.38	2.79	4.06	1.87	2.32	2.66	3.12	4.47	1.78	2.84	3.60	4.54	6.77

Table 1. Passive earth pressure coefficients $K_{p\gamma}$, K_{pq} and K_{pc}

ϕ	β/ϕ	$K_{a\gamma}$					K_{aq}					K_{ac}				
		0	1/3	δ/ϕ 1/2	2/3	1	0	1/3	δ/ϕ 1/2	2/3	1	0	1/3	δ/ϕ 1/2	2/3	1
20	0	0.490	0.459	0.449	0.442	0.436	0.490	0.460	0.450	0.444	0.441	1.400	1.503	1.553	1.603	1.712
	1/3	0.537	0.507	0.497	0.490	0.485	0.541	0.511	0.501	0.494	0.491	1.511	1.609	1.658	1.708	1.819
	1/2	0.569	0.541	0.531	0.525	0.520	0.578	0.549	0.539	0.533	0.530	1.564	1.660	1.707	1.757	1.869
	2/3	0.611	0.586	0.577	0.572	0.570	0.628	0.602	0.593	0.588	0.586	1.616	1.708	1.755	1.805	1.917
25	0	0.406	0.378	0.369	0.364	0.363	0.406	0.378	0.370	0.366	0.368	1.274	1.357	1.402	1.453	1.577
	1/3	0.451	0.423	0.415	0.410	0.410	0.456	0.427	0.419	0.415	0.417	1.387	1.463	1.507	1.558	1.685
	1/2	0.482	0.455	0.447	0.443	0.444	0.493	0.466	0.458	0.454	0.456	1.438	1.512	1.555	1.606	1.734
	2/3	0.523	0.499	0.492	0.489	0.493	0.546	0.521	0.514	0.511	0.515	1.487	1.558	1.601	1.651	1.779
30	0	0.333	0.309	0.303	0.300	0.304	0.333	0.310	0.304	0.302	0.309	1.155	1.223	1.267	1.320	1.466
	1/3	0.374	0.350	0.343	0.341	0.347	0.379	0.355	0.349	0.347	0.354	1.262	1.324	1.367	1.421	1.571
	1/2	0.402	0.379	0.373	0.371	0.379	0.416	0.392	0.386	0.384	0.393	1.310	1.368	1.411	1.464	1.615
	2/3	0.441	0.420	0.415	0.414	0.425	0.469	0.446	0.442	0.441	0.453	1.353	1.408	1.450	1.503	1.656
35	0	0.271	0.251	0.247	0.247	0.256	0.271	0.252	0.248	0.248	0.260	1.041	1.099	1.143	1.201	1.373
	1/3	0.306	0.286	0.282	0.282	0.293	0.312	0.292	0.288	0.288	0.302	1.140	1.191	1.235	1.293	1.471
	1/2	0.330	0.311	0.308	0.308	0.322	0.346	0.326	0.323	0.323	0.339	1.180	1.229	1.272	1.331	1.511
	2/3	0.365	0.347	0.345	0.347	0.364	0.398	0.378	0.376	0.378	0.397	1.216	1.262	1.304	1.363	1.544
40	0	0.217	0.202	0.200	0.202	0.215	0.217	0.203	0.201	0.203	0.219	0.933	0.983	1.029	1.092	1.295
	1/3	0.246	0.231	0.229	0.231	0.248	0.253	0.237	0.235	0.238	0.256	1.019	1.064	1.109	1.174	1.385
	1/2	0.267	0.252	0.250	0.253	0.272	0.284	0.268	0.266	0.269	0.291	1.052	1.095	1.140	1.204	1.418
	2/3	0.296	0.282	0.282	0.286	0.310	0.332	0.316	0.316	0.320	0.347	1.079	1.120	1.164	1.229	1.445

Table 2. Active earth pressure coefficients $K_{a\gamma}$, K_{aq} and K_{ac}

27

$$f_8 = \frac{L}{r_0} \left(\sin(\beta - \theta_0) + \frac{l}{r_0} \sin(\lambda - \beta) - \frac{1}{2} \frac{L}{r_0} \right)$$

29

$$\frac{l}{r_0} = \frac{-e^{\mp(\theta_1 - \theta_0) \tan \phi} \cdot \cos(\theta_1 - \beta) + \cos(\theta_0 - \beta)}{\cos(\beta - \lambda)}$$

where

28

$$\frac{L}{r_0} = \frac{e^{\mu_3(\theta_1 - \theta_0) \tan \phi} (\sin \theta_1 - \cos \theta_1 \cdot \tan \lambda) - \sin \theta_0 + \cos \theta_0 \cdot \tan \lambda}{\sin \beta \cdot \tan \lambda + \cos \beta}$$

APPENDIX 2

The user-defined functions for passive earth pressure coefficients coded in Microsoft Excel Visual Basic are as follows:

```
' Program for evaluation of Kpgama, Kpc and Kpq for rotational
' mechanism using log-spiral slip surface
Option Explicit ' All variables must be declared
' Definition of the global constants
Public Const Pi = 3.141592654
' Variables
Public Phi As Double ' internal friction angle of the soil
Public Delta As Double ' angle of friction between soil and wall
Public Lambda As Double ' inclination of the wall
Public Beta As Double ' inclination of the backfill
Public Sl_r0 As Double ' l/r0
Public CL_r0 As Double ' L/r0
' Unknown variables
Public Theta0 As Double ' first unknown angle (in radians)
Public Theta1 As Double ' second unknown angle (in radians)
' Defining the initial values
Sub Define()
Phi = Cells(5, 3).Value * Pi / 180# ' Values from the cells
Delta = Cells(6, 3).Value * Pi / 180#
Lambda = Cells(7, 3).Value * Pi / 180#
Beta = Cells(8, 3).Value * Pi / 180#
Theta0 = Cells(12, 3).Value
Theta1 = Cells(13, 3).Value
Sl_r0 = (-Exp((Theta1 - Theta0) * Tan(Phi)) * Cos(Theta1 - Beta) _
+ Cos(Theta0 - Beta)) / Cos(Beta - Lambda)
CL_r0 = (Exp((Theta1 - Theta0) * Tan(Phi)) _
* (Sin(Theta1) - Cos(Theta1) * Tan(Lambda)) - _
Sin(Theta0) + Cos(Theta0) * Tan(Lambda)) / _
(Sin(Beta) * Tan(Lambda) + Cos(Beta))
End Sub
'*****
Function f_1() As Double
Dim C1#, C2#
C1 = Exp(3# * (Theta1 - Theta0) * Tan(Phi))
C2 = 3# * (9# * (Tan(Phi)) ^ 2 + 1)
f_1 = -(C1 * (3# * Tan(Phi) * Sin(Theta1) - Cos(Theta1)) - _
3# * Tan(Phi) * Sin(Theta0) + Cos(Theta0)) / C2
End Function
'*****
Function f_2() As Double
Dim C1#, C2#
C1 = 2# * Sin(Theta0) - 2# * Sl_r0 * Sin(Lambda) + CL_r0 * Cos(Beta)
C2 = CL_r0 * Cos(Theta1 - Beta) * Exp((Theta1 - Theta0) * Tan(Phi))
f_2 = -(1# / 6#) * C1 * C2
End Function
'*****
Function f_3() As Double
f_3 = -(1# / 6#) * Sl_r0 * Sin(Theta0 - Lambda) * _
(2# * Sin(Theta0) - Sl_r0 * Sin(Lambda))
End Function
'*****
Function f_4_Kpg() As Double
Dim C1#, C2#
C1 = Cos(Delta - Lambda) * (Cos(Theta0) - Sl_r0 / 3# * Cos(Lambda))
C2 = Sin(Delta - Lambda) * (Sin(Theta0) - Sl_r0 / 3# * Sin(Lambda))
f_4_Kpg = C1 - C2
End Function
```

```

*****
Function f_4_Kpq_Kpc() As Double
Dim C1#, C2#
C1 = Cos(Delta - Lambda) * (Cos(Theta0) - Sl_r0 / 2# * Cos(Lambda))
C2 = Sin(Delta - Lambda) * (Sin(Theta0) - Sl_r0 / 2# * Sin(Lambda))
f_4_Kpq_Kpc = C1 - C2
End Function
*****
Function Kpg(c12#, c13#) As Double
Define ' Initialisation
Kpg = -(2# / Sl_r0 ^ 2#) * (f_1() - f_2() - f_3()) / f_4_Kpq_Kpc()
End Function
*****
Function Kpc(c12#, c13#) As Double
Dim f_5#, f_7#
Define ' Initialisation
' f_5 and f_7: functions f5 and f7
f_5 = Sl_r0 * Tan(Delta) / Tan(Phi) * Sin(Lambda - Theta0)
f_7 = 1# / (2# * Tan(Phi)) * (Exp(2# * (Theta1 - Theta0) * _
Tan(Phi)) - 1)
Kpc = 1 / Sl_r0 * (f_7 - f_5) / f_4_Kpq_Kpc()
End Function
*****
Function Kpq(c12#, c13#) As Double
Dim f_6#
Define ' Initialisation
' f_6: function f6
f_6 = CL_r0 * (-Sin(Theta0) + Sl_r0 * Sin(Lambda) _
- 0.5 * CL_r0 * Cos(Beta))
Kpq = -1 / Sl_r0 * f_6 / f_4_Kpq_Kpc()
End Function
*****
Function Kpq0(c12#, c13#) As Double
Dim f_8#
Define ' Initialisation
' f_8: function f8
f_8 = CL_r0 * (Sin(Beta - Theta0) + Sl_r0 * Sin(Lambda - Beta) _
- 0.5 * CL_r0)
Kpq0 = -1 / Sl_r0 * f_8 / f_4_Kpq_Kpc()
End Function

```

REFERENCES

1. COULOMB C. A. Sur une application des règles de maximis et minimis à quelques problèmes de statique relatifs à l'architecture. *Acad. R. Sci. Mém. Math. Phys.*, 1773, 7, 343-382.
2. SOUBRA A.-H., KASTNER R. and BENMANSOUR A. Passive earth pressures in the presence of hydraulic gradients. *Géotechnique*, 1999, 49, No. 3, 319-330.
3. CHEN W. F. *Limit Analysis and Soil Plasticity*. Elsevier, Amsterdam, 1975.
4. TERZAGHI K. *Theoretical Soil Mechanics*. Wiley, New York, 1943.
5. JANBU N. Earth pressure and bearing capacity calculations by generalised procedure of slices. *Proceedings of the Fourth International Conference, International Society of Soil Mechanics and Foundation Engineering*, 1957, 2, 207-213.
6. ROWE P. W. Stress-dilatancy, earth pressures, and slopes. *Journal of the Soil Mechanics and Foundation Division, ASCE*, 1963, 89, No. SM3, 37-61.
7. LEE J. K. and MOORE P. J. *Stability Analysis: Application to Slopes, Rigid and Flexible Retaining Structures. Selected Topics in Soil Mechanics*. Butterworth, London, 1968.
8. PACKSHAW S. *Earth Pressure and Earth Resistance: A Century of Soil Mechanics*. Institution of Civil Engineers, London, 1969.
9. SHIELDS D. H. and TOLUNAY A. Z. Passive pressure coefficients for sand by the Terzaghi and Peck method. *Canadian Geotechnical Journal*, 1972, 9, No. 4, 501-503.
10. SHIELDS D. H. and TOLUNAY A. Z. Passive pressure coefficients by method of slices. *Journal of the Geotechnical Engineering Division, Proceedings of the ASCE*, 1973, 99, No. SM12, 1043-1053.
11. SPENCER E. Forces on retaining walls using the method of slices. *Civil Engineering*, 1975, 18-23.
12. RAHARDJO H. and FREDLUND D. G. General limit equilibrium method for lateral earth forces. *Canadian Geotechnical Journal*, 1984, 21, No. 1, 166-175.
13. BILZ P., FRANKE D. and PIETSCH C. Earth pressure of soils with friction and cohesion. *Proceedings of the Eleventh International Conference on Soil Mechanics and Foundation Engineering, San Francisco*, 1985, 2, 401-405.
14. KUMAR, J. and SUBBA RAO, K. S. Passive pressure coefficients, critical failure surface and its kinematic admissibility. *Géotechnique*, 1997, 47, 185-192.
15. DUNCAN J. M. and MOKWA R. Passive earth pressures: theories and tests. *Journal of Geotechnical and Geoenvironmental Engineering*, 2001, 127, No. 3, 248-257.

16. CAQUOT A. and KÉRISEL J. *Tables de poussée et de butée*. Gauthier-Villars, Paris, 1948.
17. SOKOLOVSKI V. V. *Statics of Soil Media*. Butterworth, London, 1960.
18. SOKOLOVSKI V. V. *Statics of Granular Media*. Pergamon, New York, 1965.
19. GRAHAM J. Calculation of passive pressure in sand. *Canadian Geotechnical Journal*, 1971, 8, No. 4, 566–579.
20. HETTIARATCHI R. P. and REECE A. R. Boundary wedges in two-dimensional passive soil failure. *Géotechnique*, 1975, 25, No. 2, 197–220.
21. LYSMER J. Limit analysis of plane problems in soil mechanics. *Journal of Soil Mechanics and Foundation Division, ASCE*, 1970, 96, No. SM4, 1311–1334.
22. LEE I. K. and HERINGTON J. R. A theoretical study of the pressures acting on a rigid wall by a sloping earth on rockfill. *Géotechnique*, 1972, 22, No. 1, 1–26.
23. CHEN W. F. and ROSENFARB J. L. Limit analysis solutions of earth pressure problems. *Soils and Foundations*, 1973, 13, No. 4, 45–60.
24. BASUDHAR P. K., VALSANGKAR A. J. and MADHAV M. R. Optimal lower bound of passive earth pressure using finite elements and non-linear programming. *International Journal for Numerical and Analytical Methods in Geomechanics*, 1979, 3, No. 4, 367–379.
25. CHEN W. F. and LIU X. L. *Limit Analysis in Soil Mechanics*. Elsevier, Amsterdam, 1990.
26. SOUBRA A.-H., KASTNER R. and BENMANSOUR A. Etude de la butée des terres en présence d'écoulement. *Revue Française de Génie Civil*, 1998, 2, No. 6, 691–707 (in French).
27. SOUBRA A.-H. Static and seismic passive earth pressure coefficients on rigid retaining structures. *Canadian Geotechnical Journal*, 2000, 37, No. 2, 463–478.
28. SOUBRA A.-H. and REGENASS P. Three-dimensional passive earth pressures by kinematical approach. *Journal of Geotechnical and Geoenvironmental Engineering, ASCE*, 2000, 126, No. 11, 969–978.
29. KÉRISEL J. and ABSI E. *Tables de poussée et de butée des terres*, 3rd edn. Presses de l'Ecole Nationale des Ponts et Chaussées, 1990 (in French).
30. COSTET J. and SANGLERAT G. *Cours pratique de mécanique des sols. Plasticité et calcul des tassements*, 2nd edn. Dunod Technique Press, 1975 (in French).
31. CAQUOT A. *Equilibre des massifs à frottement interne. Stabilité des terres pulvérulents et cohérents*. Gauthier-Villars, Paris, 1934.

Please email, fax or post your discussion contributions to the secretary: email: mary.henderson@ice.org.uk; fax: +44 (0)20 7799 1325; or post to Mary Henderson, Journals Department, Institution of Civil Engineers, 1–7 Great George Street, London SW1P 3AA.